Development of Loaded Microspheres for Tamper-Activated Security Features

Forest Thompson; South Dakota School of Mines and Technology; Rapid City, South Dakota
Abigail McBride; South Dakota School of Mines and Technology; Rapid City, South Dakota
Linta Farooq; New Jersey Institute of Technology; Newark, New Jersey
George Wicks; Applied Research Center; Aiken, South Carolina
Grant Crawford; South Dakota School of Mines and Technology; Rapid City, South Dakota

Abstract

The ongoing technological fight against counterfeiting demands the development of new anti-counterfeiting strategies based on novel material systems. In this work, we report on a unique material system, employing porous-wall hollow glass microspheres as versatile carriers for functional security materials. To evaluate the feasibility of using these glass microspheres in anti-counterfeiting applications, several deployment configurations and processing routes were developed, whereby microsphere cargo included either (1) precursor functional materials, (2) functional materials, or (3) reactive functional materials. Microspheres were loaded using a wet vacuum technique and subsequently characterized using scanning electron microscopy, energy dispersive x-ray spectroscopy, x-ray diffraction, and spectral imaging techniques.

Introduction

Security printing and other anti-counterfeiting strategies play increasingly important roles for a variety of industries due to growing concerns of supply chains compromised by counterfeit products. The impact of counterfeiting on legitimate economic activity is well-acknowledged. The total value of counterfeit and pirated goods is conservatively projected to rise from $923 billion in 2013 to $1.90 trillion in 2022 [1]. What is perhaps less recognized is that the effects of counterfeiting on national security and public safety may be more consequential than the economic effects. Consider the routine counterfeiting of electronic components, where the number of verified incidents quadrupled between 2009 and 2011 [2]. Of the millions of low-quality counterfeit components produced, some find their way into control systems used in military, aerospace, and medical applications where high reliability and performance are critical to successful operation [3-4]. In these applications, a malfunction of a counterfeit component during operation would endanger many lives [5]. Additionally, there are fears that counterfeit components could act as Trojan horses that may be remotely disabled by malicious agents [2]. New security features that allow for improved detection and avoidance of counterfeit products are needed to prevent such outcomes.

One key to the development of more robust and effective security features is the incorporation of advanced functional materials with unique capabilities into security inks. One such material that has recently been considered for these purposes is porous-wall hollow glass microspheres (PWHGMs) [6]. PWHGMs are spherical, silica microcapsules that range in diameter from 10 to 100 μm and have shell walls with thicknesses of 1 to 2 μm. Within these thin walls, interconnected nanoscale porosity extends from the microsphere exterior to the interior which allows the interior cavities to be filled with solid or liquid cargo [7]. By encapsulating functional materials (i.e. materials with unique optical, electrical, magnetic, thermal, or chemical properties) within PWHGMs, complex, hierarchical composites can be synthesized. These loaded microspheres can then be incorporated into security inks for printed security features on products and packaging, into matrix materials for functionalized casings and coatings, or into liquid products such as paints for covert taggants. In this work, we focus on the development of composite microspheres for printable security features that can be activated by the tampering and mechanical abrasion outdated electronic components are commonly subjected to during the counterfeiting process [5].

Prior work on the application of PWHGM technology to the security printing field sought to load the microspheres with optically functional nanoparticles and to print these composite microspheres using an aerosol jet deposition system [6,8]. Low yields of nanoparticle-loaded microspheres were obtained which was attributed to the relatively large size of the nanoparticles (12-15 nm diameters) with respect to the size of the of the pore openings (12-20 nm width) that provide access to the PWHGM interiors. Here, we present a different approach to the development of composite PWHGMs for anti-counterfeiting applications using solutions containing molecules or solutes with dimensions in the sub-nanometer range, which are expected to diffuse through the wall porosity more effectively than dispersions of pre-synthesized nanoparticles. These solutions may serve as precursor functional materials, functional materials, or reactive functional materials depending on the desired end-product. This study seeks to demonstrate the feasibility of synthesizing composite microspheres containing these three forms of cargo through development of suitable processing procedures and characterization techniques.

Motivation and Procedures

PWHGMs with an average diameter of 26 μm were obtained from the Applied Research Center of Aiken, SC. The following subsections describe the motivation, loading process, and characterization of composites fabricated by combining these microspheres with functional payload materials.

Wet Vacuum Loading of PWHGMs

A wet vacuum process, based on techniques developed for hydrogen-storage applications [9], was used to load PWHGMs. Similar processes are used in industry for sealing casting porosity [10] and for loading porous catalyst supports [11], demonstrating the flexibility of this approach and its potential for application in large-scale production. The loading of porous structures with liquids is often a diffusional process. When the porosity of the structure has nanoscale dimensions and contains entrapped air, the diffusion process may take weeks to complete [11]. Wet vacuum techniques

may be used to increase the loading kinetics by removing entrapped air (to the extent possible) and encouraging liquid diffusion by imposing a pressure differential (Figure 1).

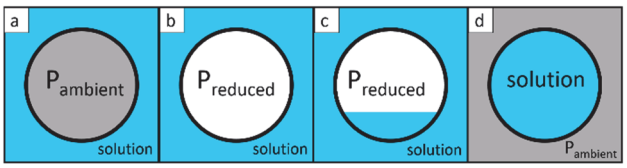

Figure 1. PWHGM wet vacuum loading process. a. PWHGM dispersed in solution at ambient pressure. b. Evacuation of ambient gasses. c. Partial transport of solution through microsphere wall porosity. d. Loading of additional solution upon restoration of ambient pressure.

Initially, dry PWHGMs are dispersed in solution through gentle mixing (Figure 1a). The microspheres contain air at ambient pressure and will typically float in solution. To partially remove the entrapped air present within the pores and interior cavity of the microspheres, the dispersion is placed within a desiccator chamber and a rotary vane vacuum pump is used to reduce the pressure within the chamber. The partial removal of air from the interior of the microspheres (Figure 1b) may initiate solution transport through the wall porosity (Figure 1c). After a prescribed soaking duration the chamber is vented to ambient pressure. The pressure difference between the microsphere interiors and the external environment drives diffusion of the solution into the interior cavity (Figure 1d). The evacuation and venting process (Figures 1b-d) may be cycled until a suitable amount of PWHGMs sink in solution, a signal that solution has displaced a significant volume of entrapped air within the microspheres. Cycling of the evacuation and venting steps is often required due to variation in wall porosity and contact with solution amongst microspheres.

Certain wet vacuum loading parameters may be varied depending on properties of the loading solution (e.g. viscosity, solute size, and vapor pressure). In this work, the variable parameters were the magnitude of reduced pressure, the soak time at reduced pressure, and the number of evacuation/vent cycles. Additional steps not included in the general wet vacuum loading procedure were also incorporated for some material systems. These case specific details will be discussed below in their respective sections.

Precursor Functional Materials

The use of nanoparticles in security printing is common due to their exceptional, functional responses to a variety of external stimuli that can be used during product authentication. While encapsulation of these materials by PWHGMs could provide enhanced or novel functionalities, the direct loading of nanoparticle dispersions has proven to be unfeasible using standard wet vacuum techniques [8]. Solution based synthesis of functional solids presents a more feasible method of loading PWHGMs. Precursor materials are more easily transported through the wall porosity and the desired payload synthesized (e.g. thermal activation or chemical precipitation) on the interior of the microsphere (Figure 2). There exists a wide variety of solution-based synthesis methods (e.g. thermal activation or chemical precipitation) for producing various functional solids meaning numerous types of composite microspheres could be fabricated and deployed in security devices. For all of these potential material systems, the encapsulation of the functional material adds security in that a stimulus, such as mechanical abrasion, is required to release the payload material to allow for its detection during product authentication.

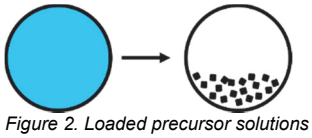

Figure 2. Loaded precursor solutions may be converted to functional solid materials within PWHGMs.

For process development and demonstration of feasibility, the synthesis of cupric oxide (CuO) structures within PWHGMs from thermal treatments of loaded aqueous copper(II) chloride ($CuCl_2$) solution was attempted [12]. Certain nanostructures of CuO have been reported to exhibit photoluminescence due to the presence of growth defects [13]. Given that PWHGM pore openings may serve as nano-templates for the nucleation and growth of nanostructures [14], the synthesis of CuO within PWHGMs has the potential to produce unique growth defects leading to photoluminescent functionality applicable to covert security features. The precursor solution was made by dissolving copper (II) chloride dihydrate ($CuCl_2 \cdot 2H_2O$) in deionized (DI) water to form a 1M aqueous solution. This solution was loaded into PWHGMs at room temperature using the wet vacuum process described previously. The reduced pressure was 30 kPa below ambient pressure and the soak duration was 0.5 h. Three evacuation/vent cycles were performed after which the PWHGMs were rinsed and filtered with deionized water using a standard vacuum filtration setup. The $CuCl_2$-loaded PWHGMs were heated in an air furnace by ramping the temperature from room temperature to 450°C at 2°C/min, followed by a 3 h hold at 450°C. Samples were then cooled to room temperature in the furnace.

For some samples, additional processing steps were taken to maximize the load factor of PWHGMs (i.e. payload volume: microsphere volume). The entire *in situ* CuO synthesis, from wet vacuum loading to thermal treatment, was repeated twice in an attempt to build up the amount of payload within the PWHGMs (Figure 3). The same wet vacuum and heat treatment parameters were utilized for both loading cycles. Intermediate wash stages were also incorporated to the loading process due to past observations of solid payload formation within wall pores and on the microsphere exterior surfaces. These observations suggested that the wet vacuum loading process may be hindered during repeated cycles due to pore blockage. Thus, after the first loading cycle, PWHGMs were soaked in 0.5 M hydrochloric acid (HCl) for 10 min to dissolve undesired CuO that may be present on the exterior surface or within the wall porosity of the PWHGMs. After this wash step, the final loading cycle was conducted.

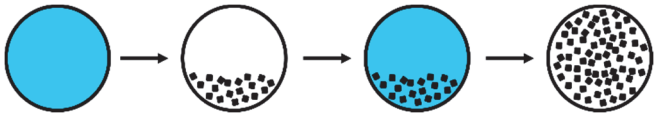

Figure 3. Increasing the load factor by repeating in situ synthesis steps until PWHGMs are filled with payload material.

Loaded PWHGMs were characterized using scanning electron microscopy (SEM), energy dispersive x-ray spectroscopy (EDS), and x-ray diffraction (XRD). The interiors of the loaded PWHGMs were analyzed using SEM by intentionally fracturing microspheres to expose their interior surfaces. EDS and XRD were used to identify the chemical composition and structure of the payload material. Comparisons were made between the PWHGMs that were loaded and heat treated once and the PWHGMs that were loaded and heat treated twice with an intermediate acid wash.

Functional Materials

Direct loading of functional materials is still possible if the dimensions of the material are small compared to the diameter of the PWHGM wall porosity. Candidate materials consist of molecules or subnanometer particles which must often remain dispersed in a solvent to exhibit functionality. Thus, the loading solution itself can be considered a functional cargo which substantially broadens the realm of material candidates for security features. The loading process is greatly simplified for this form of composite as there is no need for *in situ* synthesis. However, the need for a means of entrapping the solution within PWHGMs complicates the situation while also providing the option to impart additional functionalities (Figure 4). Similar to the solid cargo composites considered above, solution-loaded PWHGMs could respond to tampering by releasing the payload for detection. The use of functional coatings could also allow for the controlled out-diffusion of the payload after a certain period of time or when exposed to a certain environment (e.g. oxygenated atmosphere or acidic/basic pH). Such functionality would be particularly useful for the development of novel, covert taggants in liquid products, such as paints and inks. The coating aspect of this composite material development was not considered in this work, although relevant research has been conducted for the biomedical application of PWHGMs [15].

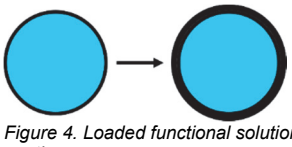

Figure 4. Loaded functional solutions may be retained within PWHGMs by coatings.

As initial steps in developing this complex material system, PWHGMs were loaded with a fluorescent solution consisting of a fluorescent molecular probe, 8-anilinonaphthalene-1-sulfonic acid (ANS), bound to a commercially available and inexpensive cow-derived protein, bovine serum albumin (BSA). Intense blue emission occurs only when ANS is bound to folded BSA and excited by ultraviolet (UV) light [16]. The fluorescent BSA/ANS solution was made by adding two drops of 0.1M aqueous ANS solution to 100 mL of 15 μM aqueous BSA solution. Wet vacuum loading was conducted at room temperature. The magnitude of the reduced pressure was 75 kPa below ambient pressure. The soak periods lasted for 60 min. Three evacuation/vent cycles were performed before the PWHGMs were filtered from the fluorescent solution using vacuum filtration. Three samples were prepared for characterization. The first was unrinsed during the filtration step while the second and third samples were rinsed with 10 mL and 50 mL of distilled water, respectively. This step was taken to analyze the retention of fluorescent solution on the interior of the PWHGMs when coatings, or other means of pore blockage, are absent. The BSA/ANS-loaded PWHGMs were analyzed by a Visual Spectral Comparator (VSC). VSC obtained the fluorescent emission spectra and the visual appearance of the three PWHGM samples when excited by 365 nm UV light.

Reactive Functional Materials

As was addressed in the previous sections, the primary benefit to creating composite material systems out of PWHGMs is the ability of the microspheres to act as protective capsules which can isolate loaded materials from the surrounding environment until released. This property of PWHGMs allows for the loading of reactive materials, which alone do not exhibit unique properties, but when exposed to an initiator material develop functional responses to stimuli, such as fluorescence under UV excitation (Figure 5). PWHGMs loaded with reactive cargo represent the most advanced form of tamper-responsive composite materials and also offer the potential for security functionality. In these systems, not only must the payload be released from the PWHGM through mechanical abrasion or out-diffusion, but the cargo must then react with an initiator before stimulated functional responses can be detected. An initiator may be present in a test solution deployed during product authentication, within the security feature as a part of a matrix material, or even within a second population of loaded PWHGMs.

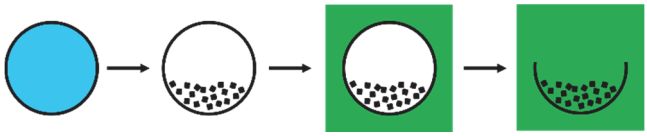

Figure 5. Loaded reactive materials may not exhibit functional responses until exposed to an initiator, illustrated here as the green matrix material.

To investigate the ability to load and then release a reactive material from within the microspheres into an environment containing an initiator, PWHGMs were loaded with ANS and then dispersed in a BSA solution. Unlike the functional solution system considered previously, fluorescence will not occur until the exterior BSA and interior ANS contact each other. PWHGMs were loaded with 0.1M aqueous ANS solution through wet vacuum loading. The reduced pressure environment was held at 75 kPa below ambient pressure. The soak duration was 30 min. Two evacuation/vent cycles were performed before the PWHGMs were vacuum filtered from the ANS solution. The ANS-loaded PWHGMs were added to 4 mL of 15 μM aqueous BSA solution while being illuminated by UV light. Then, the PWHGMs were filtered from the BSA solution, rinsed with 10 mL of distilled water, and dispersed in 4 mL of fresh 15 μM BSA solution. Again, the solution was observed under UV excitation. After 5 min, the ANS-loaded PWHGMs were placed in an ultrasonic bath while dispersed in BSA solution for 60 s. Then the vial containing the PWHGMs and BSA solution was vigorously shaken and placed under UV illumination for observation. After 5 min, the PWHGMs were filtered from the BSA solution and dried.

The response of the ANS-loaded PWHGMs to UV excitation while dispersed in BSA solution was analyzed visually and documented by photographs. Observation of fluorescence at any stage of the process would signify contact between the loaded reactive material and the surrounding initiator material. The dried PWHGMs were characterized by SEM to evaluate the effectiveness of sonication as means of breaking the microspheres to release the reactive payload.

Results and Discussion

Precursor Functional Materials

Characterization of the $CuCl_2$-loaded and heat treated PWHGMs revealed that CuO microcrystals were synthesized on the interior of the microspheres. Figure 6a is an SEM micrograph of the interior surface of a PWHGM that had been intentionally fractured for inspection of its payload. The microsphere was confirmed by SEM to be intact prior to intentional fracture. Numerous block-like structures can be observed on the interior surface of the PWHGM. EDS analysis determined that the chemical composition of the structures consisted primarily of copper and oxygen. Further, the EDS elemental map (Figure 6b) shows a clear correlation between the block-like structures and copper-concentrated regions. Similar

observations were made for numerous PWHGMs that were fractured for inspection, demonstrating the effectiveness of loading solutions rather than pre-synthesized solids. The SEM/EDS results provide strong indication that copper oxide structures were synthesized *in situ* as intended. It could not be determined from this analysis, however, if the structures were CuO, as desired, or another oxide stoichiometry such as Cu_2O.

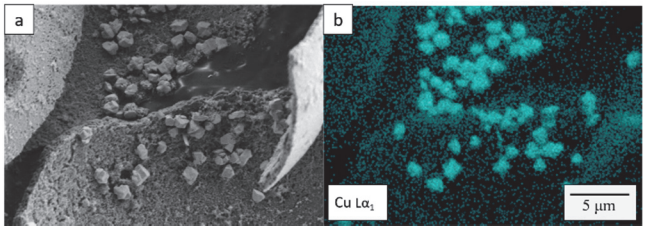

Figure 6. a. SEM secondary electron micrograph depicting block-like structures on the interior surface of a PWHGM. b. EDS copper elemental map of the same area of the PWHGM interior shown in 6a.

XRD was used to determine the copper oxide stoichiometry. Figure 7 provides an XRD pattern for PWHGMs following a single loading. The peaks identified with a star in Figure 7 are peaks that were confirmed to correspond to copper (II) oxide (CuO) based on comparison with a CuO powder XRD standard [17].

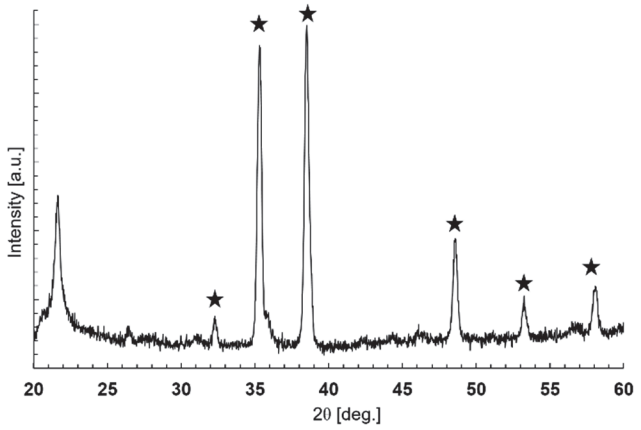

Figure 7. XRD pattern of CuO-loaded PWHGMs. Starred peaks correspond to copper(II) oxide.

The combination of the SEM, EDS, and XRD results confirms the identity of the structures as crystalline CuO. While the desired chemical composition was obtained, the size and morphology of the acquired payload limits the optical functionality of this system. Most reports of CuO luminescence are unsurprisingly related to nanostructures rather than microstructures [13]. As the synthesis method used does not permit explicit control of the size and morphology of the product, alternative synthesis methods, such as chemical precipitation of cupric salt by alkaline solutions, may be required to control the growth of CuO [18].

From inspection of Figure 6a, the CuO load factor, after one loading/conversion cycle, is quite small. Considering the limited CuO coverage observed on the surface of the fractured PWHGM, it is clear that a significant number of additional loading cycles would be required to fill the interior volume of the PWHGMs. These observations justify the investigation into the effects of multiple loading cycles on CuO load factor.

Figure 8a is a SEM image that shows a representative size distribution of loaded CuO crystals after one loading and heat treatment cycle with no acid washes. The average length of the longest dimension of the CuO crystals was determined to be 1.2 ± 0.3 µm based on analysis of 15 crystals found in two separate microspheres. Figure 8b is a SEM micrograph that shows a representative CuO structure that was found loaded within a PWHGM that underwent two loading and heat treatment cycles separated by a 0.5 M HCl soak. The average length of the longest dimension of these crystals was determined to be 3.9 ± 1.1 µm based on analysis of 15 CuO structures found in five separate microspheres.

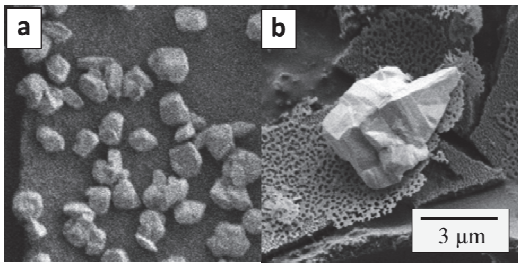

Figure 8. Representative SEM images, at identical scales, depicting the relative size of loaded CuO. a. CuO synthesized through one loading and heat treatment cycle. b. CuO synthesized through two loading and heat treatment cycles separated by an acid wash.

The repeated loading and acid washing process did not achieve the desired load factor that was portrayed in Figure 3. Rather than increasing the number of CuO structures, the size of the structures increased. This was likely caused by preferential dissolution of small CuO crystals during the acid wash followed by preferential nucleation and growth at the undissolved, larger CuO structures during the next loading cycle. Thus, the number of initial CuO structures may dictate the maximum attainable number of distinct structures regardless of the number of loading cycles. Perhaps, if the acid wash is less severe, complete dissolution of small CuO structures can be prevented and the initial number of CuO structures can be grown to occupy the total interior volume of the PWHGMs. To fill the interior with a greater number of small structures, as might be desired for tamper-activated security features, different heating ramps or precursor concentrations should be investigated, in addition to chemical precipitation methods, to determine if the nucleation and growth of the CuO structures can be better controlled.

Functional Materials

Figure 9 shows the fluorescent BSA/ANS solution that was used to load PWHGMs.

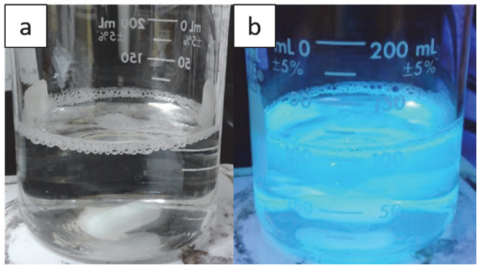

Figure 9. a. BSA/ANS solution when illuminated by white light. b. BSA/ANS solution when illuminated by a UV lamp.

In Figure 9a, the solution is illuminated under white light. The solution is transparent and no fluorescent emission is observed. In Figure 9b, the solution is illuminated by a UV lamp. Clearly, the solution takes on a bright blue color due to fluorescent emission from the BSA/ANS particles. This intense, optical response from a dilute, aqueous solution demonstrates the functionality desired from BSA/ANS-loaded PWHGMs.

The emission spectra of the BSA/ANS-loaded PWHGMs was obtained to characterize the material's fluorescence and to establish if water rinsing resulted in removal of payload solution from the microspheres. Figure 10 provides the emission spectra and visual appearance of four samples: (a) unloaded and dry PWHGMs; (b) unwashed, BSA/ANS-loaded PWHGMs; (c) BSA/ANS-loaded PWHGMs, washed with 10 mL of distilled water; and (d) BSA/ANS-loaded PWHGMs, washed with 50 mL of distilled water.

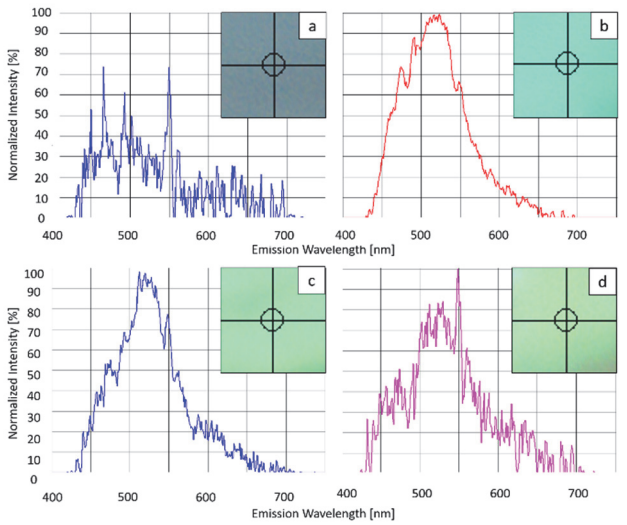

Figure 10. Emission spectra and visual appearance of unloaded and loaded PWHGMs obtained by VSC. a. Unloaded PWHGMs. b. Loaded PWHGMs, unwashed. c. Loaded PWHGMs, 10 mL distilled water wash. d. Loaded PWHGMs, 50 mL distilled water wash. Insets depicting visual appearance of emission are 0.5 mm in width.

All BSA/ANS-loaded PWHGMs exhibit a distinct blue/green emission peak at roughly 525 nm. The control sample (unloaded, dry PWHGMs) does not exhibit a clear emission peak although there is a broad and relatively weak emission centered around 500 nm. Based on these results, the presence of BSA/ANS on or within the loaded PWHGMs is confirmed. Washing clearly influences the optical response of the loaded PWHGMs as a broadening of the emission peaks and change in visual appearance occurs. Potentially this is due to an increase in BSA/ANS concentration owing to a loss of water on the interior of the microspheres. There are also potential interactions between BSA, which is known to adsorb to silica [19], with the microspheres which could influence fluorescence. Further work is needed to identify the cause of fluorescent shifts. Most critically, coatings need to be developed to effectively contain the solution on the interior of the microspheres prior to application.

Reactive Functional Materials

Figure 11 depicts the appearance of the ANS-loaded PWHGMs while dispersed in BSA solution under UV illumination. The PWHGMs in Figure 11a have been loaded, filtered, and then transferred immediately to the BSA solution. Blue fluorescent emission was observed immediately after the microspheres contacted the solution. Figure 11b shows the optical response of the dispersion when the ANS-loaded PWHGMs were washed prior to exposure to the BSA solution. A lack of blue fluorescence was observed directly although the image in Figure 11b does not present this effectively due to scattering of the incident UV light. In Figure 11c, the optical response of the loaded and washed PWHGMs is shown 5 min after sonication. Blue fluorescence was again observed but only after the microspheres soaked in solution for 5 min. Changes in fluorescence were clear during direct visual observation of the samples. However, in Figure 11, only subtle changes in color between the situations in which fluorescence was observed to have occurred (11a and 11c) and the situation in which fluorescence did not occur (11b) can be observed. This suggests more quantitative analysis is required, such as ultraviolet/visible spectroscopy (UV/Vis).

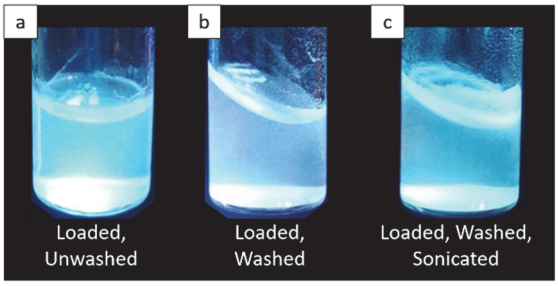

Figure 11. Comparison of optical response of ANS-loaded PWHGMs dispersed in BSA solution.

The immediate fluorescent response in Figure 11a was expected since ANS, present on the exterior of PWHGMs due to an absence of washing, was free to interact and bind with BSA in solution. The lack of fluorescent response in Figure 11b suggests that any exterior ANS was washed away and that any ANS present on the interior of the PWHGMs was kept isolated from the BSA solution by the microsphere walls. The delay in fluorescent response observed for the sample in Figure 11c was unexpected. The use of sonication and shaking was expected to fracture the PWHGMs and expose the loaded, reactive ANS to the BSA initiator. The delay in optical response suggested that the payload was not immediately exposed to the surrounding solution and that, instead, diffusion may be occurring through the porosity of intact PWHGMs.

SEM was used to analyze the state of the PWHGMs that exhibited a delayed fluorescent response. Figure 12 shows a representative SEM micrograph of the PWHGM sample on adhesive carbon tape.

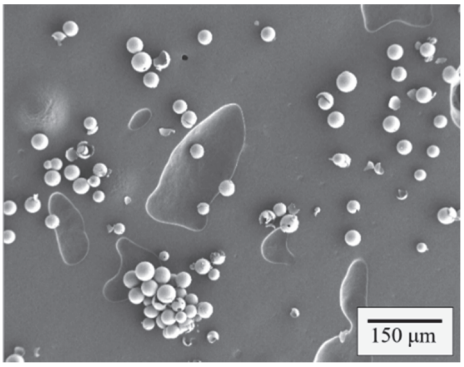

Figure 12. SEM micrograph of ANS-loaded, washed, and sonicated PWHGMs.

Some microsphere shards can be observed but the amount of PWHGMs that appear intact is substantial. This supports the theory that the time delay in fluorescent response may have been caused by insignificant microsphere fracture followed by ANS or BSA transport through the wall porosity. This points to the need for a more effective technique to evaluate reactive material release but also encourages the application of PWHGMs to security printing as it demonstrates the robustness of the microspheres when dispersed in solution and subjected to ultrasonic frequencies.

Conclusions

The studies presented here sought to demonstrate the ability to create multiple forms of PWHGM composites for use in next-generation security features that can be activated by tampering. The deployment configurations and processing routes that were studied were chosen to highlight PWHGM characteristics that can introduce new and robust security functionalities to features and product authentication methods. Specifically, the ability to load PWHGMs with precursor functional materials, functional materials, and reactive functional materials was demonstrated.

Key conclusions drawn from these studies include:

i. Solution-based loading of PWHGMs results in a yield of loaded microspheres suitable for most microscopic characterization techniques. However, improvements are required to obtain yields suitable for prototype security feature development.
ii. The CuO synthesis and BSA/ANS fluorescent emission results show that loaded solutions can be retained within PWHGMs for limited yet significant amounts of time. This suggests that both more complex *in situ* syntheses of functional solid materials and the coating of solution-loaded PWHGMs may be possible.
iii. Preliminary results from the loading of PWHGMs with reactive functional materials hint at the potential of such a system to result in complex, hierarchical security features.

The results of these preliminary studies illustrate the versatility of PWHGMs and motivate their application to anti-counterfeiting technologies. If the threats posed by counterfeit products are to be mitigated, the development of advanced functional materials, such as loaded PWHGMs, must continue.

References

[1] Frontier Economics, "The Economic Impacts of Counterfeiting and Piracy," 2016. Retrieved from https://iccwbo.org/publication/economic-impacts-counterfeiting-piracy-report-prepared-bascap-inta/

[2] IHS Markit, "Reports of Counterfeit Parts Quadruple Since 2009, Challenging US Defense Industry and National Security," 2012. Retrieved from http://news.ihsmarkit.com/press-release/design-supply-chain/reports-counterfeit-parts-quadruple-2009-challenging-us-defense-in

[3] T. Sharpe, "Counterfeit Electronic Parts in the U.S. Military Supply Chain," 2011. Retrieved from https://www.armed-services.senate.gov/imo/media/doc/Sharpe%2011-08-11.pdf

[4] The Associated Press, "Fake Electronics Becoming Military Danger," 2011. Retrieved from https://www.cbsnews.com/news/fake-electronics-becoming-military-danger/

[5] U. Guin, D. DiMase, M. Tehranipoor, "Counterfeit Integrated Circuits: Detection, Avoidance, and the Challenges Ahead," Jour. Electron. Test., vol. 30, no. 1, pp. 9-23, 2014.

[6] G. Wicks, G. Crawford, J. Keller, F. Humes, F. Thompson, "Glass Microspheres Hollow Out a Niche for Anticounterfeiting Strategies," Am. Ceramic Soc. Bull., vol. 95, no. 6, pp. 24-29, 2016.

[7] G. Wicks, "Nanostructures and 'Nanonothingness' in Unique Glass Microspheres," Int. Jour. of App. Glass Sci., vol. 4, no. 2, pp. 100-104, 2013.

[8] F. Thompson, G. Wicks, G. Crawford, "Porous-Wall Hollow Glass Microspheres for Security Printing Applications," in NIP & Digital Fabrication Conference, Portland, Oregon, 2015.

[9] L. Heung, G. Wicks, R. Schumacher, "Encapsulation of Palladium in Porous Wall Hollow Glass Microspheres," Mat. Innov. in an Emerging Hydrogen Econ. Cer. Trans., vol. 202, pp. 143-148, 2009.

[10] A. Marin, "Types of Vacuum Impregnation Processes," 2017. Retrieved from https://www.godfreywing.com/blog/bid/152308/types-of-vacuum-impregnation-processes

[11] G. Gupta, P. Shah, X. Zang, A. Saunders, B. Korgel, K. Johnston, "Enhanced Infusion of Gold Nanocrystals into Mesoporous Silica with Supercritical Carbon Dioxide," Chem. Mater., vol. 17, no. 26, pp. 6728-6738, 2005.

[12] S. Ray, "Preparation of Copper Oxide Thin Film by the Sol-Gel-Like Dip Technique and Study of Their Structural and Optical Properties," Solar Energy Mat. & Solar Cells, vol. 68, no. 3-4, pp. 307-312, 2001.

[13] X. Zhao, P. Wang, Z. Yan, N. Ren, "Room Temperature Photoluminescence Properties of CuO Nanowire Arrays," Optical Mat., vol. 42, pp. 544-547, 2015.

[14] R. Mohtadi, T. Matsunaga, K. Heung, R. Schumacher, G. Wicks, "Hollow Glass Microspheres as Micro Media for Complex Metal Hydrides Hydrogen Storage Compounds," Jour. of the S. Carolina Acad. Of Sci., vol. 9, no. 1, pp. 1-4, 2011.

[15] G. Wicks, W. Hill, P. Weinberger, "Tiny Bubbles; Composite Cocktails for Medical Applications," Int. Jour. of App. Glass Sci, vol. 7, no. 2, pp. 164-172, 2016.

[16] T. Carlson, K. Lam, C. Lam, J. He, J. Maynard, S. Cavagnero, "Naked-Eye Detection of Reversible Protein Folding and Unfolding in Aqueous Solution," Jour. of Chem. Ed., vol. 94, no. 3, pp. 350-355, 2017.

[17] ICDD File #48-1548

[18] Q. Zhang, K. Zhang, D. Xu, G. Yang, H. Huang, F. Nie, C. Liu, S. Yang, "CuO Nanostructures: Synthesis, Characterization, Growth Mechanisms, Fundamental Properties, and Applications," Prog. in Mat. Sci., vol. 60, 2014.

[19] K. Kubiak-Ossowska, K. Tokarcyzk, B. Jachimska, P. Mulheran, "Bovine Serum Albumin Adsorption at a Silica Surface Explored by Simulation and Experiment," The Jour. of Phys. Chem. B, vol. 121, no. 16, 2017.

Author Biography

Forest Thompson received his BA in physics from Colorado College (2014) and his MS in materials science and engineering from the South Dakota School of Mines and Technology (2016). Currently, he works on the development of advanced coating materials as a PhD candidate at the South Dakota School of Mines and Technology.